Bound state of the quantum dot formed at intersection of L- or T-shaped quantum wire in inhomogeneous magnetic field

Yuh-Kae Lin, Yueh-Nan Chen, and Der-San Chuu

Citation: Journal of Applied Physics **91**, 3054 (2002); doi: 10.1063/1.1446233
View online: http://dx.doi.org/10.1063/1.1446233
View Table of Contents: http://scitation.aip.org/content/aip/journal/jap/91/5?ver=pdfcov
Published by the AIP Publishing

Bound state of the quantum dot formed at intersection of *L*- or *T*-shaped quantum wire in inhomogeneous magnetic field

Yuh-Kae Lin, Yueh-Nan Chen, and Der-San Chuu[a)]
Department of Electrophysics, National Chiao Tung University, 1001 Ta Hsueh Road, Hsinchu, 30050 Taiwan

(Received 30 May 2001; accepted for publication 30 November 2001)

A quantum dot (QD) can be formed at the intersection of the symmetric or asymmetric *L*-shaped (LQW) or *T*-shaped quantum wire (TQW). The bound state energies in such QD systems surrounded by inhomogeneous magnetic fields are found to depend strongly on the asymmetric parameter $\alpha = W_2/W_1$, i.e., the ratio of the arm widths and magnetic field applied on the wire arms. Two effects of the magnetic field on the bound state energy of the electron can be obtained. One is the depletion effect which purges the electron out of the QD system. The other is to create an effective potential due to the quantized Landau levels of the magnetic field. Depletion effect is found to be more prominent in weak field region. Our results show the bound state energy of the electron in such QD system depends quadratically (linearly) on the magnetic field in the weak (strong) field region. It is also found that the bound state energy of the electron depends on the magnetic field strength only and not on its direction. A simple model is proposed to explain the behavior of the magnetic dependence of the bound state energy of the electron both in weak and strong magnetic field regions. The contour plots of the relative probability of the bound state in LQW or TQW in magnetic field are also presented. © *2002 American Institute of Physics.* [DOI: 10.1063/1.1446233]

I. INTRODUCTION

The mesoscopic structures of semiconductors have attracted intensive studies because they exhibit physical phenomena and concepts that are important in future applications of electronic devices. By mesoscopic structure, we mean the dimension of the system is less than or comparable to the phase-breaking length of the conduction electrons and much larger than the microscopic objects. Recently, quasi-one-dimensional structures, such as quantum wires attract much attention due to the enhanced confinement of the reduced dimension and the possibility of tailoring the electronic and optical properties in applications.[1–18] The physics describing the phenomena of quantum interference devices has to be explored before the development of technology. Among the structures considered, the quantum dot (QD) is one of the simpler mesoscopic systems in which the essential physics can be studied in great details. A QD can be defined by additional lateral confinements[19,20] or by applying certain magnetic fields.[21,22] The QD can also be formed at the intersection of the arms of a *L*-shaped (LQW) or a *T*-shaped (TQW) quantum wire when additional magnetic fields are applied on the arms. These QDs are quite different from the traditional quantum dots, since there remain openings in such QDs. Electrons in such QD systems are classically unbounded. However, recent experimental photoluminescence spectroscopy analyses[4–6] have manifested that there are bound states in such QDs. The existence of bound states in such QDs essentially shows the confinement effect of the mesoscopic geometry in quantum mechanical region. In addition, the stationary states of a charged particle (e.g., electron) in such QDs are affected by the applications of the inhomogeneous magnetic fields.

The exploration of the properties of bound states is a key to understand some recent optical and electrical experiments on *T*-shaped quantum wires and quantum dots.[5–7,15,18–20] The magnetophotoluminescence of *T*-shaped wires were measured recently.[9] The energy shift ΔE of photoluminescence peaks with magnetic field *B* applied perpendicular to the wire axis and parallel to the stem wire was measured. In these experiments, the information of exciton binding energy can be provided from the photoluminescence spectroscopy. However, it is unable to identify exactly the exciton binding energies unless we have the knowledge of the confinement energy of either an electron or a hole in quantum wires or quantum dots. Because they cannot be extracted directly from magneto-optical data due to the nonlinearity of the systems. In a theoretical calculation of magnetoexcitons in *T*-shaped wires,[23] the observed field dependence of the exciton states for weak confinement was reproduced, however, the diamagnetic shifts calculated from perturbation theory is fail to describe the experimental results.

In typical semiconductors, the effective masses of holes are generally anisotropic in two dimensions. Through proper variable transformation, the problem of anisotropic effective mass can be transformed formally into a problem with asymmetric geometric structure but with isotropic effective mass. However, the anisotropic effect is an intrinsic property which can be resulted only from the lattice composition, while the asymmetric effect is an extrinsic one due to the fabrication of the crystal. And this extrinsic asymmetry is often able to provide a larger preferable variation range of bound state energies whilst the intrinsic anisotropy could not. Therefore,

[a)]Author to whom correspondence should be addressed; electronic mail: dschuu@cc.nctu.edu.tw

through understanding the asymmetric effect, it might become easier to correctly tailor the devices at our desire.

In this work, we study the effects of the asymmetric geometry and the surrounding inhomogeneous magnetic fields on the electronic bound state in QDs formed in a two-dimensional *L*-shaped and *T*-shaped quantum wires. A *T*-shaped quantum wire can be obtained by first growing a $GaAs/Al_xGa_{1-x}As$ superlattice on a (001) substrate, after cleavage, a GaAs quantum wire is grown over the exposed (110) surface, resulting in a *T*-shaped region where the electron or hole can be confined on a scale of 5–10 nm. The bound state energy of a charged particle (e.g., electron) in such a quantum dot will be affected by the asymmetric geometry of the system and the applied inhomogeneous magnetic fields. Intuitively, when the confinement along one arm of the quantum wire is increased, either by decreasing the arm width or by allowing the magnetic fields surrounded the QD to change, confinement along the orthogonal arm will decrease, because squeezing the electron or hole in one arm will result in pushing the electron or hole out of the quantum wire through the other arm. These phenomena are not only interesting in physics but also have no classical correspondence. This squeezing effect has not been studied thoroughly. Furthermore, *T*-shaped semiconductor quantum wires could be exploited as three-terminal quantum interference devices, thus the study on the *L*-shaped or *T*-shaped quantum wire is also important in practical applications. Our model will be presented briefly in the next section. Results and discussions will be given in the final section.

II. FORMULATION

We consider QDs formed in a two-dimensional TQW or LQW. In our treatment the thickness in the *z* direction of our system is assumed to be very small while compared to the other two directions. Therefore, it could be practically considered as a two-dimensional system. The confinement existed in the *z* direction makes the separation of the sublevels in *z*-direction of our system to be very large while compared to those sublevels in the *x* and *y* directions of our system. The TQW and LQW are consisted of a horizontal arm and a vertical arm, lying on the $X-Y$ plane. The TQW can be divided into four uniform subregions: a horizontal arm with a width of W_1 (region I) to which a magnetic field B_1 is applied perpendicularly, another horizontal wire with a width of W_1 (region II) to which a magnetic field B_2 is applied perpendicularly, a vertical arm with a width of W_2 to which a magnetic field B_3 is also applied perpendicularly and an intersection region with an area of $W_1 \times W_2$ (region IV), as shown in Fig. 1(a). For simplicity, the boundaries are assumed to be a hard-wall confinement potential, leading to the formation of a magnetically confined cavity in which the confinement of electron is enhanced. The case of LQW [shown in Fig. 1(b)] can be regarded as a transformation of TQW in which the arm 2 is cutoff and only three subregions are left. The transverse potential inside the TQW or LQW is assumed to be zero. For further studies, the magnetic fields are assumed to be uniform in each individual subregion and is zero in the intersection region (region IV). Within the framework of effective mass approximation, the Schrödinger equation of an electron in TQW system (the system of LQW is just the special situation of TQW) under an inhomogeneous magnetic field can be expressed as:

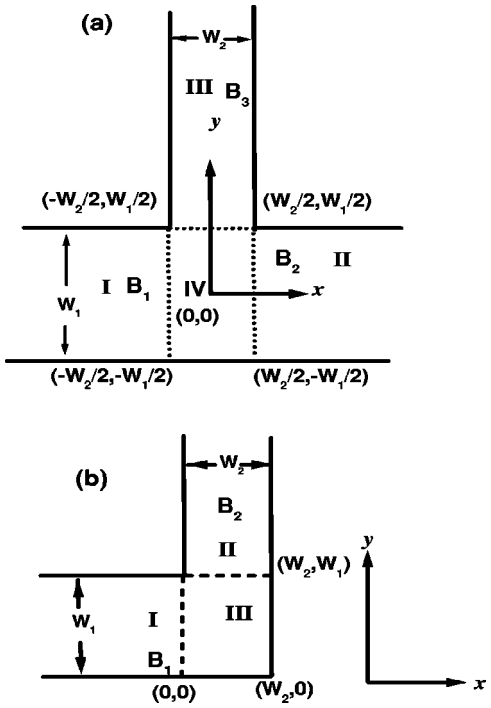

FIG. 1. The illustrations of the geometries of QDs in (a) TQW and (b) LQW systems.

$$\left[-\frac{(\mathbf{p}-\mathbf{qA}(\mathbf{x},\mathbf{y}))^2}{2m^*}+V_c(x,y)\right]\Psi(x,y)=E\Psi(x,y), \quad (1)$$

where m^* and q are the effective mass and the charge of the particle, $V_c(x,y)$ is the confinement potential, and **p** is the momentum, **A(x,y)** is the vector potential associated with the magnetic fields. To solve the equation, the Landau gauge is chosen for the vector potential in different subregions as

$$\mathbf{A(x,y)}=\begin{cases}[0,B_1(x+0.5W_2)]=(-B_1y,0)+\nabla B_1(x+0.5W_2)y, & \text{in region I;}\\ [0,B_2(x-0.5W_2)]=(-B_2y,0)+\nabla B_2(x-0.5W_2)y, & \text{in region II;}\\ [-B_3(y-0.5W_1),0]=(0,B_3x)-\nabla B_3x(y-0.5W_1), & \text{in region III;}\\ (0,0), & \text{in region IV.}\end{cases} \quad (2)$$

The origin of the coordinate system is chosen at the center of the intersection region. It can be noted that this form of gauge guarantees the continuity of the vector potential at each interface.

The wave function of the bound state n of an electron for the different four regions can be expressed as follows:

$$\Psi_n^{\mathrm{I}} = e^{-i(x+0.5W_2)yeB_1/\hbar}\left[\sum_m r_{mn} e^{ik_m^{\mathrm{I}}(x+0.5W_2)}\Phi_m^{\mathrm{I}}(y)\right]$$

in region I;

$$\Psi_n^{\mathrm{II}} = e^{-i(x-0.5W_2)yeB_2/\hbar}\left[\sum_m t_{mn} e^{ik_{mn}^{\mathrm{I}}(x-0.5W_2)}\Phi_m^{\mathrm{II}}(y)\right]$$

in region II; (3)

$$\Psi_n^{\mathrm{III}} = e^{ix(y-0.5W_1)eB_3/\hbar}\left[\sum_m s_{mn} e^{ik_m^{\mathrm{II}}(y-0.5W_1)}\Phi_m^{\mathrm{III}}(x)\right]$$

in region III;

and

$$\Psi_n^{\mathrm{IV}} = \sum_j \{f_j(y)[a_{jn}\sin k_j'(x-0.5W_2) + b_{jn} \times \sin k_j'(x+0.5W_2)] + c_{jn} g_j(x)\sin k_j''(y+0.5W_2)\} \tag{4}$$

in the region IV, where $f_j(y)$ and $g_j(x)$ represent the transverse wave functions of electron in mode j at zero field in horizontal and vertical arms, respectively, and can be formally expressed as

$$f_j(y) = \sqrt{\frac{2}{W_1}}\sin\left(\frac{j\pi}{W_1}y\right), \quad -0.5W_1 \leqslant y \leqslant 0.5W_1, \tag{5}$$

$$g_j(x) = \sqrt{\frac{2}{W_2}}\sin\left(\frac{j\pi}{W_2}x\right). \quad -0.5W_2 \leqslant x \leqslant 0.5W_2, \tag{6}$$

and the nominal wave numbers are $k_j' = [k^2 - (j\pi/W_1)]^{1/2}$ and $k_j'' = [k^2 - (j\pi/W_2)]^{1/2}$, respectively. And k_m^i, $i = \mathrm{I,II,III,}\cdots$ are the nominal longitudinal wave vectors of the mth mode in regions I, II, or III, respectively. They are either real for escaping states or pure imaginary for bound states. a_{jn}, b_{jn}, c_{jn}, r_{mn}, s_{mn}, and t_{mn} are the expansion coefficients in their own regions. In Eq. (3), we expanded our wave function in terms of a set of oscillating functions. The oscillating (exponential) functions are used as the expansion basis. The reason that we include more than one term in the wave function is due to the requirement of the convergence of the complicated situations induced by asymmetry and magnetic field. Therefore, the final wave function contains a linear combination of the oscillating (exponential) functions and behaves like a sharper decaying function than the pure exponential function in regions I, II, and III. By this way, the subscript n can be cast aside because we are only concerned with certain bound state. After we substitute Eqs. (3) into the Schrödinger equation, the transverse wave function Φ_m of the mth mode is found to satisfy the following individual one-dimensional Schrödinger equations of an electron with the bound state energy $E = \hbar^2 k^2/2m^*$ and charge $q = -e$:

$$\left[\frac{d^2}{dy^2} + k^2 - \left(k_m^{\mathrm{I}} - \frac{eB_1}{\hbar}y\right)^2 + V_c(y)\right]\Phi_m^{\mathrm{I}}(y) = 0 \tag{7}$$

in region I,

$$\left[\frac{d^2}{dy^2} + k^2 - \left(k_m^{\mathrm{II}} - \frac{eB_2}{\hbar}y\right)^2 + V_c(y)\right]\Phi_m^{\mathrm{II}}(y) = 0 \tag{8}$$

in region II, and

$$\left[\frac{d^2}{dx^2} + k^2 - \left(k_m^{\mathrm{III}} + \frac{eB_3}{\hbar}x\right)^2 + V_c(x)\right]\Phi_m^{\mathrm{III}}(x) = 0 \tag{9}$$

in region III. Where $k = \sqrt{(2m^*E/\hbar^2)}$, and V_c is the confinement potential. From the earlier equations, one can see that the magnetic fields are introduced into the relevant Schrödinger equations as an additional effective potential. It is obvious that each term in Eqs. (4) satisfies automatically the Schrödinger equation. Therefore, Eqs. (7), (8), and (9) have to be solved independently. We expand the transverse wave functions Φ_m^i, $i = \mathrm{I,II,III}$ in terms of the sets of complete basis at zero field as

$$\Phi_m^{\mathrm{I}}(y) = \Sigma_j \xi_{mj}^{\mathrm{I}} f_j(y), \text{ in region I;}$$

$$\Phi_m^{\mathrm{II}}(y) = \Sigma_j \xi_{mj}^{\mathrm{II}} f_j(y), \text{ in region II;}$$

$$\Phi_m^{\mathrm{III}}(x) = \Sigma_j \xi_{mj}^{\mathrm{III}} g_j(x), \text{ in region III.} \tag{10}$$

The expansion involves an infinite number of terms. However, in reality, this sum must be truncated at certain large number to achieve a desired accuracy. We are in the situation to find simultaneously the values of the wave vectors k_m^{I}, k_m^{II}, and k_m^{III} for a given energy E satisfying Eqs. (7), (8), and (9), respectively. Unfortunately, this is not straightforward since the equations are not eigen equations in k^i, where $i = \mathrm{I,II,III}$ for a given E because E is not linear in k^i. This difficulty can be resolved by converting Eqs. (7), (8), and (9) into eigen equations in k^i by the following transformation:

$$\eta_m^{\mathrm{I}}(y) = k_m^{\mathrm{I}}\Phi_m^{\mathrm{I}}(y), \tag{11}$$

$$\eta_m^{\mathrm{II}}(y) = k_m^{\mathrm{II}}\Phi_m^{\mathrm{II}}(y), \tag{12}$$

$$\eta_m^{\mathrm{III}}(y) = k_m^{\mathrm{III}}\Phi_m^{\mathrm{III}}(y). \tag{13}$$

Equations (7) and (8) can now be recast formally as

$$\begin{bmatrix} 0 & 1 \\ \dfrac{\partial^2}{\partial y^2} + \dfrac{2m^*E_F}{\hbar^2} - \left(\dfrac{y}{l_{B_i}}\right)^2 & \dfrac{2y^2}{l_{B_i}} \end{bmatrix}\begin{bmatrix} \Psi_m^i(y) \\ \eta^i(y) \end{bmatrix} = k_m^i \begin{bmatrix} \Psi_m^i(y) \\ \eta^i(y) \end{bmatrix} \tag{14}$$

in region i, $i = \mathrm{I,II}$. By substituting x for y, and $-B_3$ for B_i, we have matrix equation in region III. With the help of the earlier expanded basis and the transformation for a given energy E_F, we obtain a set of eigen-wave numbers $\{k_m^{\mathrm{I}}\}$, $\{k_m^{\mathrm{II}}\}$, and $\{k_m^{\mathrm{III}}\}$, all the expansion coefficients in Eqs. (3) and (4), and the eigen-wave functions $\{\Phi_m^{\mathrm{I}}(y)\}$, $\{\Phi_m^{\mathrm{II}}(x)\}$, and $\{\Phi_m^{\mathrm{III}}(x)\}$. By requiring the wave function and their normal derivatives to retain continuity at each interface, and performing tedious numerical processes, the eigen energy E and eigen wave function Ψ are then obtained.

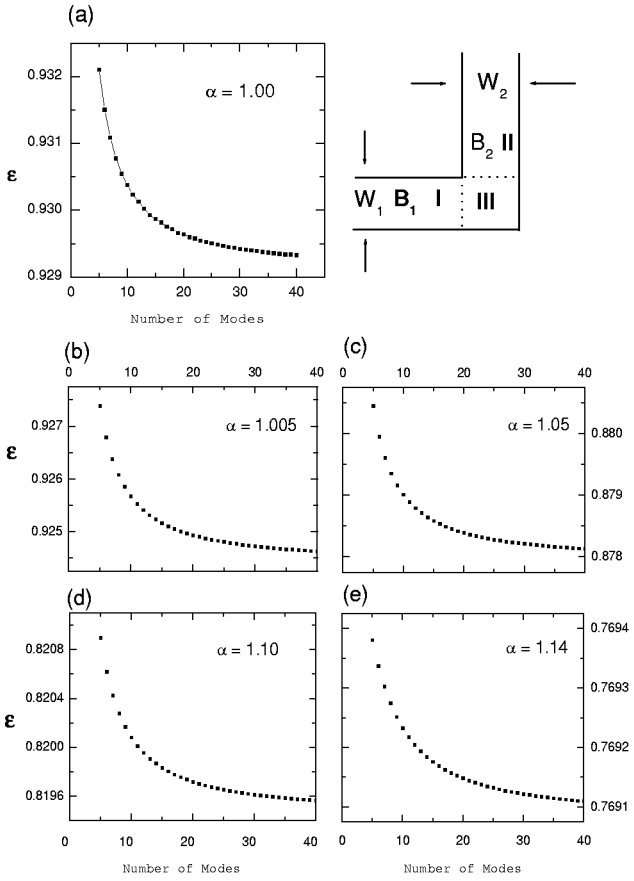

FIG. 2. The convergence tests of the number of modes for LQW system for different α. (a) $\alpha=1.00$, (b) $\alpha=1.005$, (c) $\alpha=1.01$, (d) $\alpha=1.05$, and (e) $\alpha=1.14$. Even for large $\alpha=1.14$, our calculation converges rapidly.

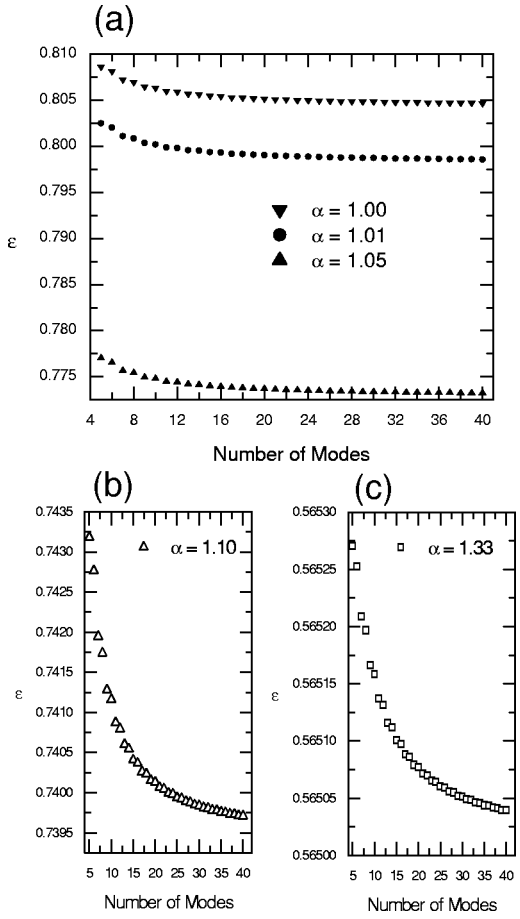

FIG. 3. The convergence tests of the number of modes for T-shaped QW system for (a) solid down-triangle for $\alpha=1.00$, solid circle for $\alpha=1.01$, and solid up-triangle for $\alpha=1.05$, (b) open up-triangle for $\alpha=1.10$, (c) open square for $\alpha=1.33$. Even for large $\alpha=1.33$, our calculation converges rapidly.

III. RESULTS AND DISCUSSIONS

A. The convergence of numerical calculations

By using the mode matching technique, we are able to obtain the bound state energy of an electron in the quantum dot formed at the intersection of the arms of a L-shaped or a T-shaped quantum wire when magnetic fields are applied on the arms. In order to make the numerical computation become feasible, the numbers of modes in the wider arms are properly considered while the ratios of arm widths is nearly zero or extremely large. Moreover, different number of modes for each arm is also carefully considered. To make sure whether our numerical calculation is reliable or not, the tendency of convergence for different number of modes included in our calculation is presented in Fig. 2 for an LQW with some typical α values. Figure 2(a) presents the result for the symmetric case, i.e., $\alpha=1$ or $W_2=W_1$. And Figs. 2(b), 2(c), 2(d), and 2(e) are the obtained results for cases of $\alpha=1.005$, $\alpha=1.05$, $\alpha=1.10$, and $\alpha=1.14$, respectively. The tendency of convergence for different number of modes included in our calculation for TQW system is shown in Fig. 3. As shown in Fig. 3(a), three cases are presented: solid down-triangle represents the result obtained by using $\alpha=1$ (i.e., $W_2=W_1$), solid circle presents the result for $\alpha=1.01$, and solid up-triangle for $\alpha=1.05$. Fig. 3(b) and (c) present the results obtained for $\alpha=1.10$ and $\alpha=1.33$, respectively. It is noticeable that our calculations converge rapidly even in the case with large value of α though we just included same number of modes in each region. Our results agree well with previous works.[24–27]

B. The bound states in QDs at zero field

Figure 4 presents the variation of the calculated bound state energies of an electron in a LQW as a function of arm ratio α. For clarity, the bound state energy of the electron is expressed in terms of the dimensionless quantity $\epsilon=E/E_1$ throughout this article, where $E_1=(\hbar^2\pi^2/2m^*W_1^2)$ is the first subband level in arm 1 (region 1). One can note from the figure that the bound state energy of the electron becomes smaller as the arm ratio α becomes larger. For $\alpha=1$ (i.e., $W_1=W_2$), i.e., a symmetric L-shaped quantum wire, we have $r_m=t_m$ at zero magnetic field, the bound state energy of the electron is obtained as $0.92964E_1$. For asymmetric geometries, the calculated bound state energy ϵ goes down and behaves like the curve of $1/\alpha^2$ as the asymmetric parameter α is increased larger than 1.14. A deviation from the curve of $1/\alpha^2$ is observed in the region of $\alpha\leqslant 1.14$ as can be seen in the inset of Fig. 4. The result can be ascribed to the fact that the bound state energy of the electron matches the subband energy of arm 2 due to the lateral confinement of region II.

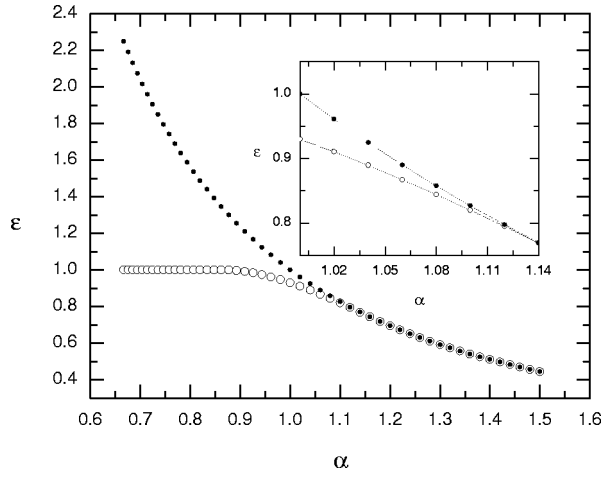

FIG. 4. The bound state energy ϵ vs the asymmetric ratio $\alpha = W_2/W_1$ at zero magnetic field strength. Open circle is our result. The dotted line is the curve of $1/\alpha$ as a guide to eyes. $E_1 = (\hbar^2\pi^2)/(2m^*W_1^2)$ is the first threshold energy of arm 1 (the region I).

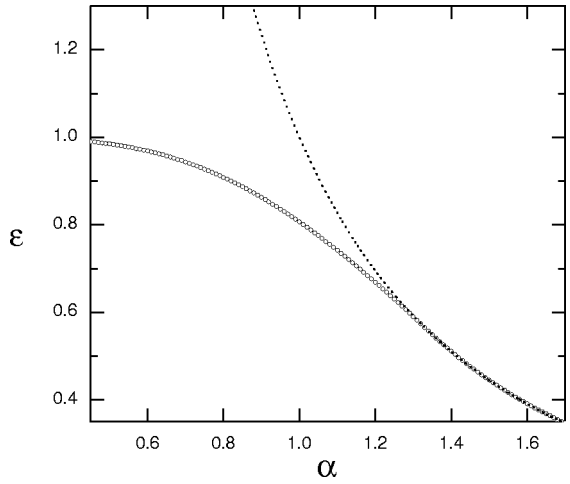

FIG. 6. The bound state energy ϵ of a TQW plotted in unit of E_1 as a function of α. The bound state energy of the electron approaches to unity for $\alpha \ll 1$ and can be approximately expressed by the curve $1/\alpha^2$ for $\alpha \geqslant 1.33$

Since in this circumstance, $1/\alpha^2(\pi/W_1)^2$ is just equal to $(\pi/W_2)^2$, which is the first subband level of the vertical wire. As the width W_2 becomes larger and larger, this energy level becomes lower and lower, and gradually coincides with the bound state energy level of the electron. Thus the electron is unable to be bounded in the corner region any more. This can be understood by the clue exhibited in the distribution of the probability density of the electrons. The probability density of electrons in the LQW can be evaluated by summing up over all terms

$$\rho(x,y) = \sum_{n=1}^{N} |\Psi_n(x,y)|^2. \tag{15}$$

Figure 5 shows the contour plots of the probability density distribution of the bound states for several α values in an asymmetric LQW system. The distributions are normalized to their own maxima for simplicity, and the most inner contour curve possesses the highest probability density. In the case of $\alpha = 1$, the contour of the probability density distribution reflects a mirror symmetry due to its symmetric geometry as can be seen from Fig. 5(a). The electron piles up at the corner region as the localized state is formed. In these cases, the probability density distribution decays exponentially in the arm regions, such that the electron is unable to go far away from the corner. One can also note from Fig. 5, as the structure asymmetry of the LQW becomes prominent, e.g., as α increases from 1.005 in (b) to 1.05 in (c) and finally 1.10 in (d), the probability density distribution gradually extends to the wider arm region. As the asymmetry becomes more obviously, the peak of the electron probability density distribution transmits eventually out of the corner region providing the electronic energy is larger than the bottom of the subband of the wider arm. However, if the energy of the electron state is less than or just equal to the subband bottom, the electron is still bounded inside the corner and does not move to the right or to the left. Therefore, this state cannot transmit in the arm and does not contribute to the conductance. Hence, it consequently results in valleys or dips near the transmission thresholds.[17]

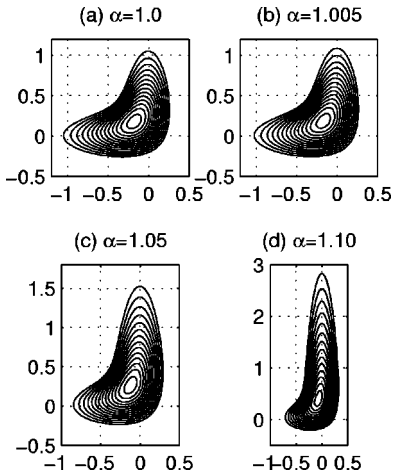

FIG. 5. The probability density distributions of electron in LQW for different asymmetric parameter α. (a) $\alpha = 1$, (b) $\alpha = 1.005$, (c) $\alpha = 1.01$, (d) $\alpha = 1.05$, and (e) $\alpha = 1.1$. All distributions are normalized to its maximum value for simplicity.

Now let us consider the case of a TQW. For a TQW, if we change the ratio $\alpha = W_2/W_1$, we do not change its image symmetry. Thus, it can be expected that at least one bound state can exist in TQW no matter how large the width of the transverse arm is. Figure 6 shows the bound state energy of the electron in a TQW as a function of α. One can see from the figure that bound state energy approaches unity as the width of the vertical arm becomes very small, and behaves like a curve of $1/\alpha^2$ while the value α becomes larger. This is similar to the case of a LQW. The reason of this result can be understood intuitively that the wave function of the electron is purged out of the vertical arm when it becomes very narrow and thus the wave function is almost squeezed inside the longitudinal arm, therefore, the energy of this state is close to the first threshold energy E_1 of the horizontal arm with a width of W_1. This bound state of the electron exists as long

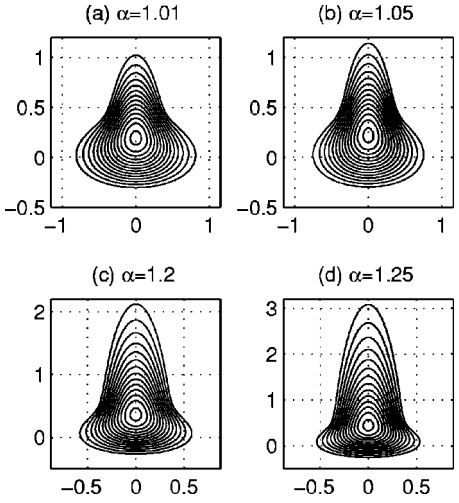

FIG. 7. The contour plots of the relative probability of the bound state of an electron in an asymmetric TQW.

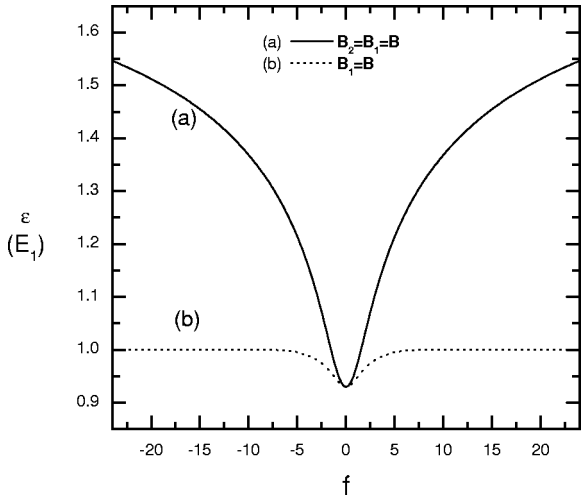

FIG. 9. The bound state energy ϵ vs the field strength f. (a) For both arms being acted by the magnetic fields in LQW system. (b) For only one arm being acted by the magnetic fields. The dimensionless field strength f is normalized by E_1.

as the vertical arm is infinite long, and is expected to disappear owing to the effect of leakage if the arms is finite in length.

Actually, the bound state energies of electrons of the QDs are slightly higher than $1/\alpha^2$ for large α, and also slightly lower than 1 for small α. The bound state of the electron thus always exists no matter how large the ratio α is, except for one of the arms has finite length. One can observe this result from the contour plots of the probabilities depicted in Fig. 7 for $\alpha \geqslant 1$ and Fig. 8 for $\alpha < 1$.

It often involves anisotropic factors in semiconductor systems. The anisotropic Hamiltonian for an anisotropic heavy hole at zero field is given by

$$\hat{H} = -\left[\frac{\hbar^2}{2m_x^*}\frac{\partial^2}{\partial x^2} + \frac{\hbar^2}{2m_y^*}\frac{\partial^2}{\partial y^2}\right] + V(x,y). \tag{16}$$

Let $\tilde{y} = (m_y^*/m_x^*)^{1/2} y$, then Eq. (16) can be rewritten as

$$\hat{H} = -\frac{\hbar^2}{2m_x^*}\left[\frac{\partial^2}{\partial x^2} + \frac{\partial^2}{\partial \tilde{y}^2}\right] + V(x,\tilde{y}). \tag{17}$$

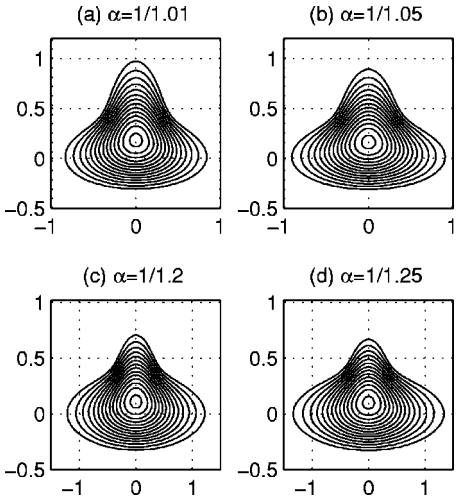

FIG. 8. The contour plots of the relative probability of the electron bound state in an asymmetric TQW.

Comparing with Eqs. (7) and (8), we have the same Schrödinger equations if we change the variable y into $\tilde{y}$. The anisotropic factor $\alpha = (m_y^*/m_x^*)^{1/2}$ is large as 1.348 for a typical GaAs system if we adapt the values: $m_{hh[110]} = 0.69 m_0$ and $m_{hh[001]} = 0.38 m_0$.[5] This value gives rise to the result that the hole is extremely anisotropic distributed in TQW structure. However, it should be still bounded as we already mentioned.

C. Effects of magnetic fields on the electronic bound state in a QD

For simplicity and clarity, the QDs are considered to be formed on symmetric two-dimensional LQW and TQW systems, that is only the case of $W_2 = W_1$. The calculated bound state energies of the electrons in the QD formed in LQWs under the magnetic fields are plotted as functions of the field strength $f = \hbar\omega_c / E_1$, as depicted in Fig. 9(a) for case of both arms and in Fig. 9(b) for case of only one arm in the LQW system subjected to magnetic field, where ω_c is cyclotron frequency of the electron. One can observe that the bound state always exists when the magnetic field is applied to both arms. The energy level of the electron in this case is monotonically increased while the magnetic field is increased. In the contrast, curve (b) shows the energy of the bound state of the electron is pushed up by the applied magnetic field, and then it goes up to E_1. Thus, the electron can escape via the field free arm.

For the symmetric TQW, there are two main configurations of the applications of magnetic fields. The case of symmetrically applying magnetic fields to the system includes three types which are shown in Fig. 10. In Fig. 10, curve (a) displays the confinement energy versus the field strength when all arms are acted by the same magnetic field B, curve (b) displays the energy versus the field strength when the two horizontal arms are acted by the same magnetic field, and curve (c) displays that only the vertical arm is acted by the magnetic field. The same quadratic dependence of magnetic

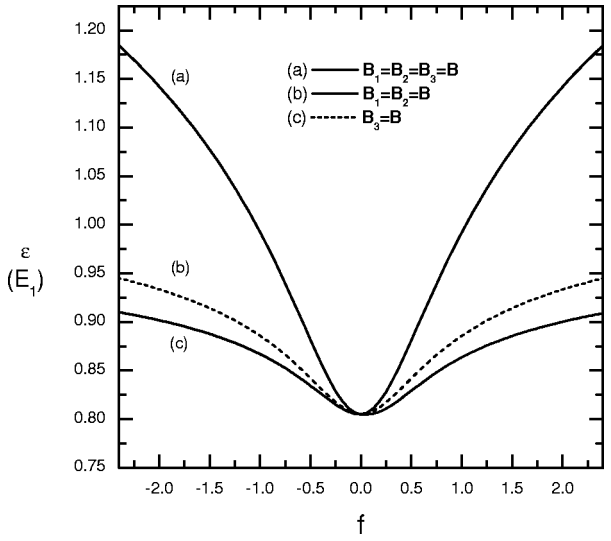

FIG. 10. The bound state energy ϵ of *T*-shaped QW as a function of the field strength *f*. Curve (a) for all arms being acted by magnetic fields. The field strength *f* is normalized by E_1. Curve (b) for the horizontal arms being acted by magnetic fields, and curve (c) for only vertical arm being acted by magnetic field. The dimensionless field strength *f* is normalized by E_1.

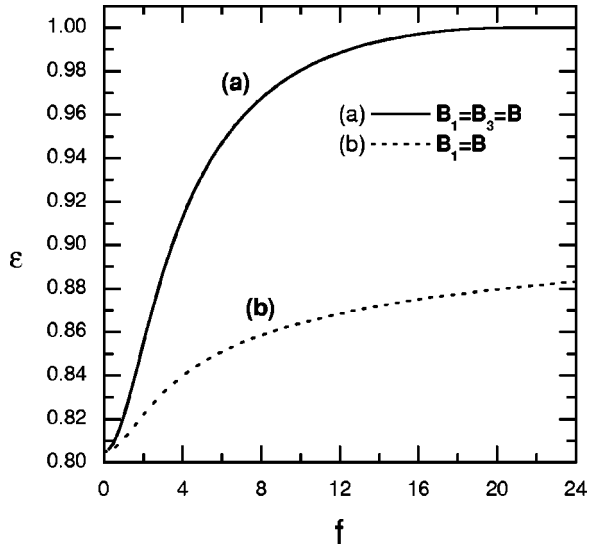

FIG. 12. The bound state energy ϵ of T-shaped QW as a function of the field strength *f*. Curve (a) for the region I (or region II) and region III being acted by the same magnetic field. Curve (b) for only region I (or region II) being acted by magnetic field. The dimensionless field strength *f* is normalized by E_1.

field of the bound state energy of the electron is revealed again for the weak field strength, and the linear dependence appears in the strong field region as the case of LQW. For these symmetric configurations of magnetic field, the bound state always exists. It is found that the more arms are acted by the magnetic field, the higher energy of the bound state of the electron is obtained due to the stronger depletion effect. The quadratic dependence region is wider if the depletion effect is smaller, as shown in curves (a), (b), and (c) of Fig. 10. Obviously, the bound state level of the electron in a TQW system locates deeper than that in a LQW, that is, the TQW system has a weaker confinement potential than the LQW system. This causes a deviation of bound energies about $0.12E_1$. We also calculated several relative probability contours of the bound state of the electron under the magnetic fields as displayed in Fig. 11.

For the case of inhomogeneous magnetic field applying on the TQW, the energy levels of electron are shown in curves (a) and (b) of Fig. 12. Curve (a) of Fig. 12 presents the case of the magnetic fields applying to region I (or region II) and region III of the TQW system, and curve (b) of Fig. 12 presents that of the magnetic field applying to region I (or region II) only. These curves consist of the former result that the more regions are acted by magnetic fields, the higher energy of the bound state of the electron are obtained. And from Fig. 12(a), it can be observed that the energy of the bound state approaches E_1 for a higher magnetic strength. This is a similar consequence of the conclusion obtained in the LQW system. The behavior is also found from curve (b) of Fig. 12, however, its value approaches the energy of the QD in a symmetric LQW system. Both curves (a) and (b) of Fig. 12 show quadratic feature for weaker magnetic field regions due to the depletion effect of magnetic field. Compare curves (a) and (b) of Fig. 12, one can notice that a wider quadratic region directly reflects the weaker depletion effect of the magnetic fields.

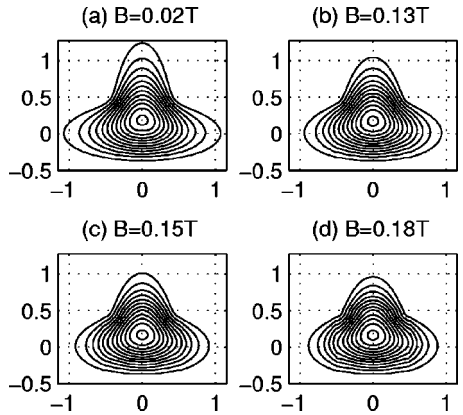

FIG. 11. The contour plots of the relative probability of the electron bound state in TQW under the magnetic field.

The external perpendicular magnetic fields introduce a depleting effect on electrons and add an extra potential surrounding the QD. From Eqs. (7), (8), and (9), one can observe that the effective potentials introduced by the magnetic fields are *k* dependent. For the bound state, these effective potentials are complex due to the pure imaginary $\{k\}$. Therefore, one cannot easily figure out the effective potentials.

One can expect intuitively that the magnetic field adds the lowest Landau level $\hbar\omega_c/2=\hbar eB/2m^*$ directly to the quantum dot system (in the corner region) an extra potential. Such levels are added into the wire regions surrounding the QD. However, the field plays another role due to the essential physics of the magnetism. Qualitatively, one can understand the effect induced by the magnetic field on the bound state of the electron by considering an one-dimensional shallow quantum well with finite height U_0. In the limit of shallow well, there is only one bound state exists in the well. Its level energy is given by $E_0=U_0-(m^*W^2/2\hbar^2)U_0^2$,[28] which

is near the top of the well. Let us consider that if the potential height is changed to $U_0+1/2\hbar\omega_c$ due to the application of the external magnetic field, then how does the bound state energy of the electron change? This is not quite intuitive to figure out. First, it is easy to see that the variation of the state level depends linearly on the potential height, i.e.,

$$\frac{\partial E_0}{\partial U_0}=1-\frac{m^*W^2}{\hbar^2}U_0. \tag{18}$$

To take into account the depletion effect of the magnetic field, which effectively suppress the envelop of the electron wave, the variation of the state level is assumed as

$$\frac{\partial E_0}{\partial W}=-\frac{m^*W}{\hbar^2}U_0^2. \tag{19}$$

Obviously, once we need to take the well shrunk into account, the quadratic form of the dependence of magnetic field has to be considered also. This remarkable simple model manifests the essential important effect of geometric scale in quantum behavior, and also manifests one of the essential properties of magnetism at the same time. However, in the strong magnetic field strength region, the shrinking of the geometric scale is no longer prominent, because the electron wave function is squeezed to a certain local area. And there is fewer probability left in the arms, therefore there is less influence of the magnetic field on the electron. Thus, the energy of bound state of the electron depends simply on the added effective potential, such that it seems likely to depend linearly on the magnetic field in the high field strength region.

IV. SUMMARY

The asymmetry parameter, which is defined as $\alpha=W_2/W_1$, plays an important role in the formation of a QD. The asymmetry parameter strongly affects the bound state of an electron in a QD. When the asymmetry parameter α increases, the bound state energy of the electron is lower as expected. On the other hand, when the applied magnetic field increases, the bound state level of the electron is pushed higher and higher and the electron begins to be unbounded if there is an arm with finite length which offers a passway for electron to leak out. Generally, the bound state level of an electron in the QD formed in a TQW system is lower than that in LQW system. This fact reflects the weaker confinement of the geometry. It is found that the magnetic field also affects the bound state, even though the spin of the electron is not taken into account. Parabolic dependence of the bound state energy of the electron in weak field region on the field strength is understood as a result of the depletion effect. In the contrast, linear dependence in high field region is found to be resulted from the additional effective potential due to the magnetic field.

ACKNOWLEDGMENT

This work is supported partially by National Science Council, Taiwan under the Grant No. NSC90-2112-M-009-018.

[1] Y.-C. Chang, L. L. Chang, and L. Esaki, Appl. Phys. Lett. **47**, 1324 (1985).
[2] F. Sols, M. Macucci, U. Ravaili, and K. Hess, J. Appl. Phys. **66**, 3892 (1989); F. Sols and M. Macucci, Phys. Rev. B **41**, 11887 (1990).
[3] D. S. Chuu, C. M. Hsiao, and W. N. Mei, Phys. Rev. B **46**, 3898 (1992); C. M. Hsiao, W. N. Mei, and D. S. Chuu, Solid State Commun. **81**, 807 (1992).
[4] S. N. Walck, T. L. Reinecke, and P. A. Knipp, Phys. Rev. B **56**, 9235 (1997).
[5] S. Glutsch, F. Bechstedt, W. Wegscheider, and G. Schedekbeck, Phys. Rev. B **56**, 4108 (1997).
[6] W. Langbein, H. Gislason, and J. M. Hvam, Phys. Rev. B **54**, 14595 (1996).
[7] H. Gislason, C. B. Sǿrensen, and J. M. Hvam, Appl. Phys. Lett. **69**, 800 (1996).
[8] H. Gislason, W. Langbein, and J. M. Hvam, Appl. Phys. Lett. **69**, 3248 (1996).
[9] T. Someya, H. Akiyama, and H. Sakaki, Phys. Rev. Lett. **74**, 3664 (1995); T. Someya, H. Akiyama, and H. Sakaki, Appl. Phys. Lett. **66**, 3672 (1995).
[10] A. Yacoby, H. L. Stormer, N. S. Wingreen, L. N. Pfeiffre, K. W. Baldwin, and K. W. West, Phys. Rev. Lett. **77**, 4612 (1996).
[11] R. Šordan and K. Nikolić, Appl. Phys. Lett. **68**, 3599 (1996).
[12] L. Burgnies, O. Vanbésien, and D. Lippens, Appl. Phys. Lett. **71**, 803 (1997).
[13] G. Goldoni, F. Rossi, and E. Molinari, Appl. Phys. Lett. **71**, 1519 (1997); **69**, 2965 (1996); G. Golodoni, F. Rossi, E. Molinari, and A. Fasolino, Phys. Rev. B **55**, 7110 (1997); F. Rossi, G. Goldoni, and E. Molinari, Phys. Rev. Lett. **78**, 3527 (1997).
[14] M. Yoshita, H. Akiyama, T. Someya, and H. Sakaki, J. Appl. Phys. **83**, 3777 (1998); T. Someya, H. Akiyama, and H. Sakaki, Phys. Rev. Lett. **76**, 2965 (1996); H. Akiyama, T. Someya, M. Yoshita, T. Sakai, and H. Sasaki, Phys. Rev. B **57**, 3765 (1998).
[15] D. Brinkmann and G. Fishman, Phys. Rev. B **56**, 15211 (1997).
[16] J. L. Bohn, Phys. Rev. B **56**, 4132 (1997).
[17] B.-Y. Gu, Y. K. Lin, and D. S. Chuu, J. Appl. Phys. **86**, 1013 (1999); K.-Q. Chen, B.-Y. Gu, Y. K. Lin, and D. S. Chuu, Int. J. Mod. Phys. B **13**, 903 (1999).
[18] M. Grundmann, O. Stier, and D. Bimberg, Phys. Rev. B **58**, 10557 (1998).
[19] C.-T. Liang, I. M. Castleton, J. E. F. Frost, C. H. W. Barnes, C. G. Smith, C. J. B. Ford, D. A. Ritchie, and M. Pepper, Phys. Rev. B **55**, 6723 (1997).
[20] C.-T. Liang, M. Y. Simmons, C. G. Smith, G. H. Kim, D. A. Ritchie, and M. Pepper, Phys. Rev. Lett. **81**, 3507 (1998).
[21] L. Solimany and B. Kramer, Solid State Commun. **96**, 471 (1995).
[22] H.-S. Sim, K.-H. Ahn, K.-J. Chang, G. Ihm, N. Kim, and S.-J. Lee, Phys. Rev. Lett. **80**, 1501 (1998).
[23] G. W. Bryant and Y. B. Band, Phys. Rev. B **63**, 115304 (2001).
[24] R. L. Schult, D. G. Ravenhall, and H. W. Wyld, Phys. Rev. B **39**, 5476 (1989).
[25] J. P. Carini, J. T. Londergan, K. Mullen, and D. P. Murdock, Phys. Rev. B **46**, 15538 (1992); **48**, 4503 (1993).
[26] J. Goldstone and R. L. Jaffe, Phys. Rev. B **45**, 14100 (1992).
[27] J. Wang and H. Guo, Appl. Phys. Lett. **60**, 654 (1992).
[28] L. D. Landau and E. M. Lifshitz, *Quantum Mechanics: Non-Relativistic Theory*, 3rd ed. (Pergamon, NY, 1977), problem 2 in §22, p. 65.